BOSTON UNIVERSITY

GRADUATE SCHOOL OF ARTS AND SCIENCES

Dissertation

MEASUREMENT OF THE ANOMALOUS MAGNETIC MOMENT OF THE POSITIVE MUON TO .SOMETHING PARTS PER BILLION

by

NICHOLAS BRENNAN KINNAIRD

B.S., University of Texas at Austin, 2013
B.S., University of Texas at Austin, 2013
M.A., Boston University, 2016

Submitted in partial fulfillment of the

requirements for the degree of

Doctor of Philosophy

2019

Approved by

First Reader

B. L. Roberts, PhD
Professor of Physics

Second Reader

R. M. Carey, PhD
Professor of Physics

Third Reader

J. P. Miller, PhD
Professor of Physics

Dedication

I dedicate this thesis to

Acknowledgments

Here go all your acknowledgments. You know, your advisor, funding agency, lab mates, etc., and of course your family.

As for me, I would like to thank Jonathan Polimeni for cleaning up old LaTeX style files and templates so that Engineering students would not have to suffer typesetting dissertations in MS Word. Also, I would like to thank IDS/ISS group (ECE) and CV/CNS lab graduates for their contributions and tweaks to this scheme over the years (after many frustrations when preparing their final document for BU library). In particular, I would like to thank Limor Martin who has helped with the transition to PDF-only dissertation format (no more printing hardcopies – hooray !!!)

The stylistic and aesthetic conventions implemented in this LaTeX thesis/dissertation format would not have been possible without the help from Brendan McDermot of Mugar library and Martha Wellman of CAS.

Finally, credit is due to Stephen Gildea for the MIT style file off which this current version is based, and Paolo Gaudiano for porting the MIT style to one compatible with BU requirements.

Janusz Konrad

Professor

ECE Department

MEASUREMENT OF THE ANOMALOUS MAGNETIC MOMENT OF THE POSITIVE MUON TO .SOMETHING PARTS PER BILLION

(Order No.)

NICHOLAS BRENNAN KINNAIRD

Boston University, Graduate School of Arts and Sciences, 2019

Major Professor: B. L. Roberts, Professor of Physics

ABSTRACT

Have you ever wondered why this is called an *abstract*? Weird thing is that its legal to cite the abstract of a dissertation alone, apart from the rest of the manuscript.

Contents

List of Tables

List of Figures

List of Abbreviations

ppm	.....	parts per million
ppb	.....	parts per billion
SM	.....	Standard Model
SiPM	.....	Silicon Photo-Multiplier

Chapter 1

Introduction

1.1 Background

1.1.1 Definitions

1.1.2 Experiment History

1.2 Theory

1.2.1 QED

1.2.2 Weak

1.2.3 Hadronic

1.2.4 BSM

Chapter 2

Muon g-2 at Fermilab, E989

2.1 Principle Technique

In a magnetic field, particles will orbit at the cyclotron frequency

$$\omega_c = -\frac{Qe}{\gamma m}B, \tag{2.1}$$

and their spins will turn at the precession frequency

$$\omega_s = -g\frac{Qe}{2m}B - (1-\gamma)\frac{Qe}{\gamma m}B, \tag{2.2}$$

where $Q = \pm 1$ and $e > 0$. The difference between these two frequencies gives

$$\omega_a = \omega_s - \omega_c = -\frac{g-2}{2}\frac{Qe}{m}B = -a_\mu\frac{Qe}{m}B, \tag{2.3}$$

a measureable frequency that is directly proportional to the property of significance, a_μ . By measuring the spin difference frequency for muons and the magnetic field, a_μ can be determined. In the presence of an electric field, which is necessary to store the muon beam, this expands to

$$\vec{\omega_a} = -\frac{Qe}{m}[a_\mu\vec{B} - (a_\mu - \frac{1}{\gamma^2-1})(\vec{\beta}\times\vec{E})], \tag{2.4}$$

where now the measurable quanties are vector quantities. Finally, for realistic cases of muon momentum is non-orthogonal to the magnetic field, the spin difference fre-

Figure 2·1: test caption

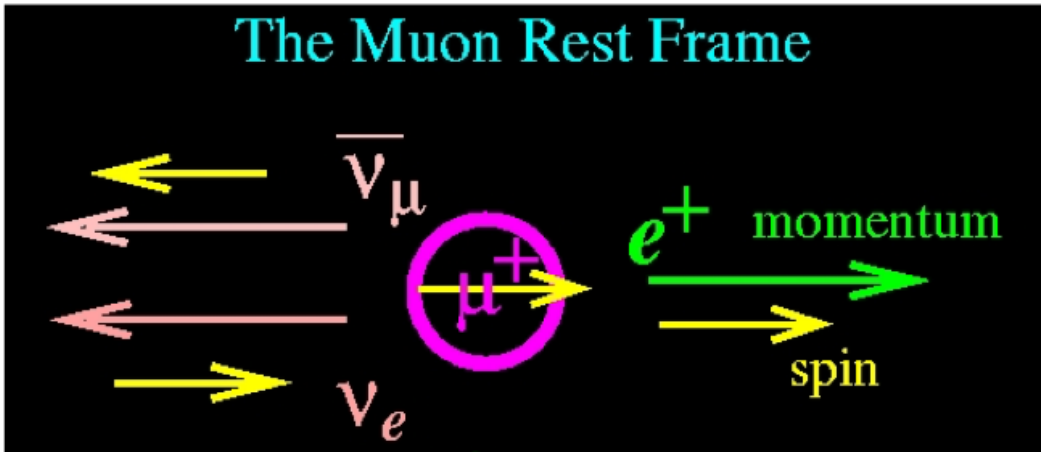

quency becomes

$$\vec{\omega}_a = -\frac{Qe}{m}[a_\mu \vec{B} - a_\mu(\frac{\gamma}{\gamma+1})(\vec{\beta}\cdot\vec{B})\vec{B} - (a_\mu - \frac{1}{\gamma^2-1})(\vec{\beta}\times\vec{E})]. \tag{2.5}$$

If the motion of the muons is largely perpendicular to the magnetic field, then the second term is small and can be corrected for. If the particles have a momentum of approximately 3.09 GeV/c, the so called "magic momentum," then the third term is small and can be corrected for.

In order to measure the spin difference frequency of the muons, a clever technique is used. Decay muons in the pion rest frame are 100% polarized due to the conservation of angular momentum and the fact that the decay neutrino must have a specific helicity. Within a pion beam then the highest and lowest energy decay muons are polarized. Muons will decay to positrons with a lifetime of about 2.2 μs, and the positrons with the highest energies will be correlated with the muon spin, a so called "self-analyzing" decay. The single available decay state for a maximum energy positron illustrates this in Figure 2·1

-explain the physics -explain how we get at the physics with our ring and detectors don't measure all decay positrons

By injecting a large ensemble of muons and

Careful with spin vs polarization

2.2 Detector Systems

2.2.1 Calorimeters

Electromagnetic calorimeters measure the times and energies of decay positrons as they curl inward from the storage region. There are 24 calorimeters located symmetrically around the inside of the ring in close proximity to the vacuum chamber, as shown in Figure **??**. They lie close to the storage region in order to measure a large fraction of the total number of observable decay positrons, including the high energy decay positrons which curl inward only slightly more than the muons themselves do. Because they are in close proximity to the storage region and by extension the magnetic field, the calorimeters must be non-magnetic in order to avoid perturbing the magnetic field. Each calorimeter consists of 54 channels of PbF_2 crystals arrayed in a 6 high by 9 wide array, which measure Cerenkov light emitted by the impinging positrons as they pass through the crystals [1]. (Picture of single calo and its crystals here.) Each crystal is 2.5 x 2.5 x 14 cm^3. The light is read out by large area silicon photo-multiplier (SiPM) sensors.

In order to determine a_μ to the precision goal, there are modest requirements on the performance of the calorimeters. They must have a relative energy resolution of better than 5% at 2 GeV, in order for proper event selection [2]. They must have a timing resolution of better than 100 ps. The calorimeters must be able to resolve multiple incoming hits through temporal or spatial separation at 100% efficiency for time separations of greater than 5 ns in order to reduce the pileup systematic error due to the high rate. Finally, the gain of the measured hits must be stable to $< 0.1\%$ over a 200 μs time period within a fill, and unaffected by a pulse arriving in the same

channel a few nanoseconds earlier. The long term gain stability over a time period of order seconds must be $< 1\%$.

(I've condensed quite a bit this section from the TDR - is that okay?)

To satisy these requirements SiPM sensors were chosen over PMTS...

and is wrapped in black Tedlar® foil

2.2.2 Laser System

For the gain, there is a laser system...

[4]

2.2.3 Template Fitting

Chapter 3

Magnetic Field Measurement

3.1 Trolley

Chapter 4

Straw Tracking

4.1 Straw Tracking Intro

Move a lot of this stuff into a tracker section in the hardware/experiment part

The Muon $g-2$ Experiment at Fermilab uses straw tracking detectors to measure decay positron trajectories for the purpose of determining the muon beam distribution and its characteristics. By fitting these tracks and extrapolating back to the average decay point, the beam can be characterized in a non-destructive fashion. This is important because of the need for matching the average observed magnetic field of the decaying muons and their resulting decay positron directions which result in the ω_a frequency, as seen in

$$\vec{\omega}_a = \frac{e}{m}[a_\mu \vec{B} - a_\mu(\frac{\gamma}{\gamma+1})(\vec{\beta}\cdot\vec{B})\vec{B} - (a_\mu - \frac{1}{\gamma^2-1})(\vec{\beta}\times\vec{E})]. \tag{4.1}$$

The trackers are also useful for determining general beam diagnostics as well as the pitch correction and to a lesser extent the electric field correction, terms 2 and 3 in Equation 4.1 respectively. The tracking analysis can be done independently of, or in tandem with, the calorimeters. Cross-checking separately for pileup removal, hit verification, etc. is a powerful tool. Combining them in order to provide the muon distribution that the calorimeters directly see for the ω_a calculation is perhaps the most important role of the tracker. (An EDM analysis needs to be done separately.) It is worth noting that there is a large percentage of tracks hitting the calorimeters

that hit zero or only a small number of tracking modules, which this Geane fitting code is not capable of handling. With three trackers, approximately 5% of decaying muons will result in measureable positron tracks assuming no pileup in the tracker, many of which do not hit the nearest calorimeter. Note that the integration of the two detector systems in the code (tracker-calo matching) has just recently been initiated, DocDB 7514.

Each tracker module consists of 4 layers of 32 straws with a stereo angle of 7.5 degrees, the first two "U" layers oriented with the tops of the straws at a greater radial position, and the second two "V" layers oriented with the bottoms of the straws at a greater radial position. A tracking module is shown in Figure 4·1. There are 3 tracker stations located at the 0th, 12th, and 18th sections of the ring, counting clockwise from the top most point of the ring where the inflector resides. Figure **??** shows this. (Station 18 was installed for the commissioning run, with station 0 planned for the fall. Station 12 might or might not be installed sometime in the future.) Each station consists of 8 tracking modules arranged in a staircase pattern that follows the curvature of the ring as seen in Figure 4·2. Further hardware and electronics information regarding the trackers will be omitted in this document.

Because of the proximity of the trackers to the muon beam, they will lie within a region of varying magnetic field. The radial field of the trackers rises from 0 Tesla at the outer ends to roughly .3 Tesla at the inner top and bottom ends, and the vertical field drops approximately 50% from the storage dipole field of 1.451 Tesla. Shown in Figures 4·3 and 4·4 is the location of the tracker with respect to the horizontal and vertical fields respectively. These large field gradients over the tracking detector region and the long extrapolation distance back to the muon decay point are special to Muon $g-2$. This is one of the main motivations for using the Geane (Geometry and Error Propagation) fitting algorithm and routines, which has direct access to the

Figure 4·1: Shown is a picture of one of the many tracking modules used in the Muon $g-2$ experiment. The first layer of straws with a stereo angle of 7.5 degrees can be seen, with the other 3 straw layers hiding behind it. The beam direction is roughly into the page in this picture, to the left of the end of the module, and this view is what the decay positrons will see.

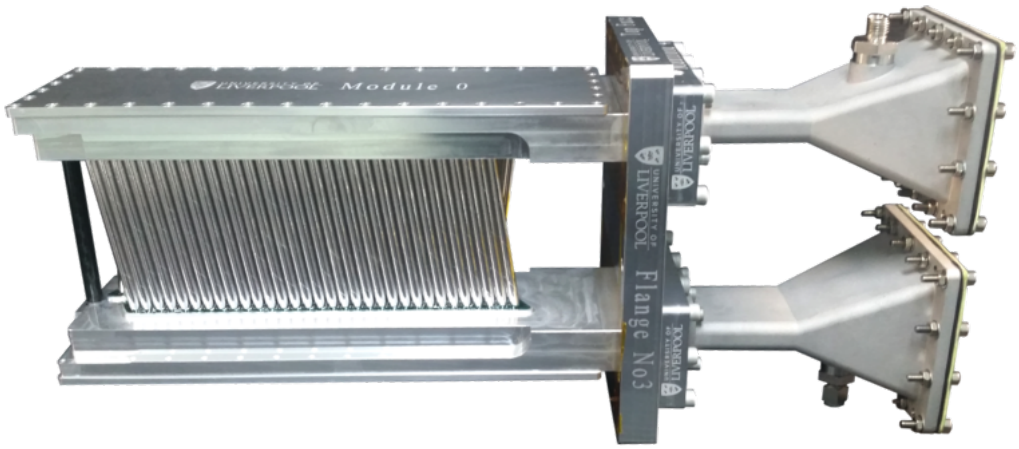

field.

The Geane fitting routines originated in Fortran with the EMC collaboration, and was used in the precursor E821 experiment as well as the PANDA experiment with some success [3], [5]. (I'm not actually aware of a useful reference for it's use in E821, and there are some other instances of its use as well in other experiments. In E821 there was a single tracking chamber which was never put to full use.) The core error propagation routines were at some point added to Geant4 under the error_propagation directory which is included in all default installs. The tracking code strengths lie with its direct implementation and access to the Geant4 geometry and field, and its ability to handle the field inhomogeneties. The Geane fitting algorithm code which makes use of the Geant4 error propagation routines follows the structure of [3] and is detailed in the Formalism section in this paper. It is a relatively straight forward least squares global χ^2 minimization algorithm.

Figure 4·2: Tracker modules are arranged in the shown staircase pattern. In green and dark blue is the edge of the vacuum chamber (where the dark blue identifies the modification that was made to the old vacuum chambers), and it can be seen that vacuum chamber walls lie at the ends of the outside tracking modules. The position of a calorimeter can be seen in cyan at the right. The dark red spots are the locations of the outside magnet pole tips. From the shown geometry one can see that many positrons will hit either the tracker or the calorimeter but not both due to the acceptance differences.

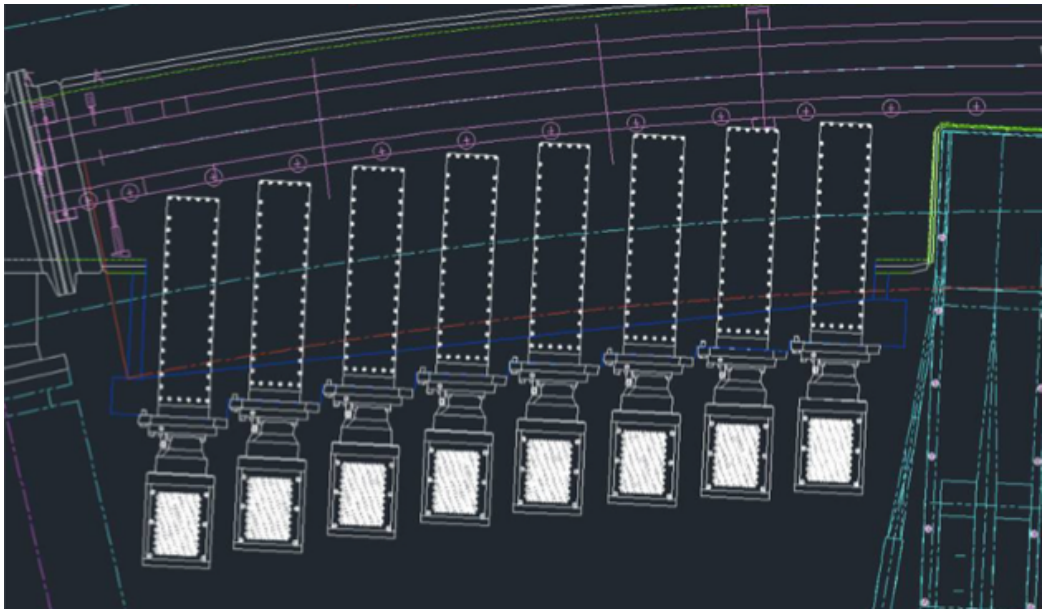

Figure 4·3: Shown is the vertical field of the $g-2$ magnet in and around the storage region as calculated in Opera 2D. The center of the storage region lies at 7.112 m along the x axis. The black box shows the rough location of the tracker with respect to the field (size exaggerated slightly). It can be seen that there is a large inhomogeneity within the tracker space, goring from left to right.

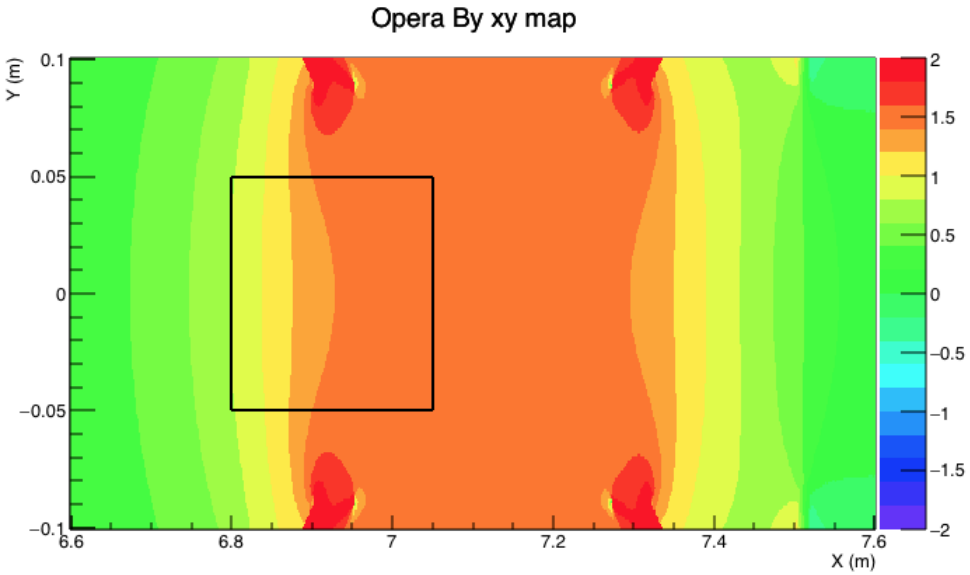

Figure 4·4: Shown is the radial field of the $g-2$ magnet in and around the storage region as calculated in Opera 2D. The center of the storage region lies at 7.112 m along the x axis. The black box shows the rough location of the tracker with respect to the field (size exaggerated slightly). It can be seen that there is a large homogeneity at the inner upper and lower ends compared to the right center. The shape of the pole pieces and tips can readily be seen.

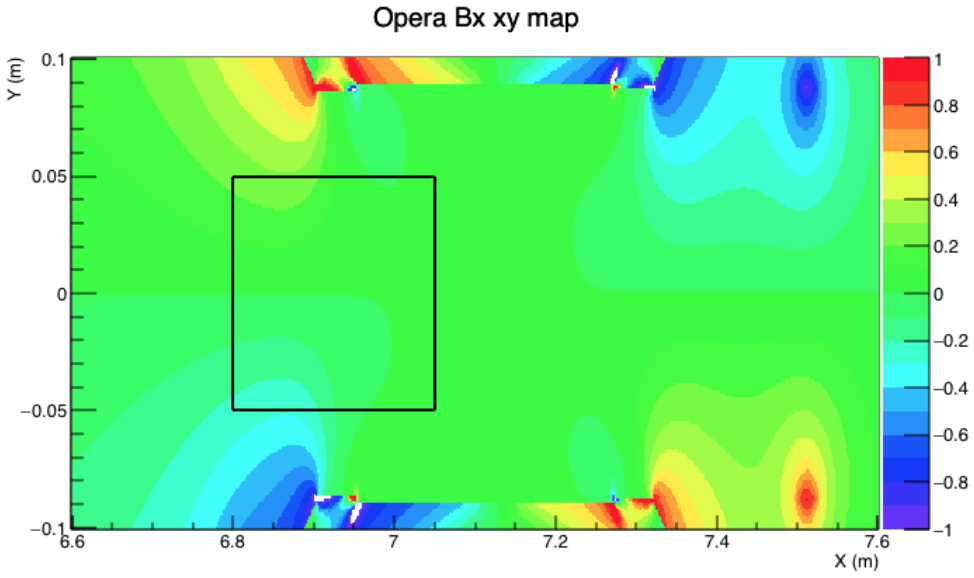

4.2 Track Finding

4.3 Track Fitting

4.4 Track Extrapolation

Chapter 5

ω_a Measurement

5.1 Data

5.2 Spectra Making

5.2.1 Clustering

5.2.2 Histogramming

5.3 Fitting

5.4 Systematic Errors

Chapter 6

Conclusion

6.1 Final Value

test4

Appendix A

Proof of xyz

This is the appendix.

Bibliography

[1] A. T. Fienberg et al. "Studies of an array of PbF_2 Cherenkov crystals with large-area SiPM readout". In: *Nucl. Instrum. Meth.* A783 (2015), pp. 12–21. DOI: 10.1016/j.nima.2015.02.028. arXiv: 1412.5525 [physics.ins-det].

[2] J. Grange et al. "Muon (g-2) Technical Design Report". In: (2015). arXiv: 1501.06858 [physics.ins-det].

[3] V. Innocente, M. Maire, and E. Nagy. "GEANE: Average tracking and error propagation package". In: *MC 91: Detector and event simulation in high-energy physics. Proceedings, Workshop, Amsterdam, Netherlands, April 8-12, 1991*. 1991, pp. 58–78. URL: http://innocentonnice.web.cern.ch/innocentonnice/napoli99/geane_manual.ps.

[4] J. Kaspar et al. "Design and performance of SiPM-based readout of PbF_2 crystals for high-rate, precision timing applications". In: *JINST* 12.01 (2017), P01009. DOI: 10.1088/1748-0221/12/01/P01009. arXiv: 1611.03180 [physics.ins-det].

[5] Lia Lavezzi. "The fit of nuclear tracks in high precision spectroscopy experiments". pp. 57-86. PhD thesis. Pavia U., 2007. URL: http://bamboo.pv.infn.it/doc/L_Lavezzi.pdf.

CURRICULUM VITAE

Joe Graduate

Basically, this needs to be worked out by each individual, however the same format, margins, typeface, and type size must be used as in the rest of the dissertation.